



Effect of bone marrow mesenchymal stem cells on cisplatin-induced cytotoxicity in parotid gland of rats (Histological and Ultrastructural studies)

Ahmed Saad Abdelaziz¹, Hany Abd-Elhamid Sherif², and Abd Elnasser Abd El mawla³

¹*Faculty of Dental Medicine, Al-Azhar University, Boys, Cairo, Egypt.*

²*Faculty of Dental Medicine, Al-Azhar University, Boys, Cairo, Egypt.*

³*Faculty of Dental Medicine, Al-Azhar University, Boys, Cairo, Egypt.*

Abstract

The current study was implemented to assess the therapeutic efficacy of bone marrow mesenchymal stem cells on parotid glands following cytotoxicity induced by cisplatin administration in rats. The study employed a sample of 36 adult male Sprague-Dawley rats. The samples were categorized into two groups. The control group (6 rats) received 0.5ml phosphate-buffered saline. The experimental group was divided into two subgroups; subgroup (A), the cisplatin group, (15 rats) was administered a solitary intraperitoneal injection of the cisplatin medication at 10 mg/kg. Subgroup (B) BMMSc group (15 rats) was administered the same dose of cisplatin as subgroup A. On day three following cisplatin administration, 5×10^5 BMMSCs suspended in 0.5 ml of PBS were injected intraparotid. After cisplatin injection and BMMSc administration rats were sacrificed according to different time intervals (7 and 21 days) for histological and ultrastructural analysis. The stem cell-treated group exhibited superior histological and ultrastructural characteristics. This investigation proved that BMMSCs can improve the histological and ultrastructural changes of parotid glands induced by cisplatin administration.

Keywords: Parotid glands, cisplatin, stem cells.

Full length article *Corresponding Author, e-mail: Ahmedsaadabdelazizmostafa.209@azhar.edu.eg

1. Introduction

Cisplatin (cis-diammine dichloro-platinum II (CP)) is a chemotherapeutic drug that is highly effective and extensively employed in the treatment of numerous head, neck, and ovarian malignancies [1]. The mechanism by which CP induces DNA damage is due to its capacity for crosslinking with the purine bases on the DNA. Cisplatin exerts additional cytotoxic effects on tumor cells via mitochondrial disruption, disrupted cellular transport mechanisms, and diminished the activity of ATPase [2]. CP exhibits potent chemotherapeutic properties; however, its cytotoxicity and lack of selectivity towards cancer cells, which also impacts healthy tissues, may result in undesirable side effects [1]. Stem cell therapy is an effective treatment for many clinical conditions. BMMSCs have been shown to promote tissue regeneration in numerous organs, including the kidneys [3] and ovaries [3,4], subsequent cisplatin-induced cytotoxicity. Additionally, they demonstrated the capacity to enhance the proliferation capability of damaged cells across various tissues [5-7]. The potential mechanism

for this involves the paracrine secretion of cytokines and growth factors, such as hepatocyte growth factor (HGF), interleukin-6 (IL-6), and vascular endothelial growth factor (VEGF), as well as anti-apoptotic factors, including caspase-3 [5].

2. Material and methods

2.1 Animals and experimental design

The animal handling and the application of the procedure were carried out at the animals' house of Veterinary Medicine Cairo University and approved by the local ethical committee Ref. No.592/1786. The animals were caged individually with free access to water and food. The present study was carried out on adult male Sprague Dawley rats with an average age of around 2 months old, and their weight measured 200-250 gm.

2.2 Animal grouping

The animals were divided randomly into two main groups:-

2.2.1 Group I

(Control group, 6 rats) A parotid gland injection of 0.5 ml of PBS was administered to Group I.

2.2.2 Group II

Experimental Group, divided into two subgroups.

2.2.2.1 Subgroup (A)

The cisplatin group, 15 rats) will receive a single intraperitoneal injection of cisplatin drug (10 mg/kg) [8].

2.2.2.2 Subgroup (B)

(BMMSC group, 15 rats) received the dose of cisplatin used in subgroup A, then BMMSCs (5×10^5 cells) [9] suspended in 0.5 ml of PBS were injected intra-parotid at day 3 after cisplatin administration. After 7 and 21 days from cisplatin administration and BMMSC injection, the rats will be anesthetized, sacrificed and the parotid gland will be dissected out and prepared for:
- Haematoxylin and Eosin staining are routine stains.
- Transmission electron microscope examination, TEM was carried out using JEOL JEM 1010 TEM at 70kv at the regional center for mycology and Biotechnology (RCMB), Alazhar University.

2.3 Isolation of bone marrow mesenchymal stem cells

BMMSCs were obtained from the long bones of three adult experimental rats weighing between 100 and 150 g [10].

2.3.1 Image analysis

The images were analysed by mounting an Olympus® digital camera on an Olympus® microscope equipped with a 1/2 X photo adaptor and a 40 X objective to digitize the slides. The obtained images were analyzed on a computer powered by an Intel® Core I7® processor employing Video Test Morphology® software (Russia). The software included a dedicated built-in routine for area measurements. Two slides were utilized per rat, and five random fields were extracted from each slide to determine intracytoplasmic vacuolation.

2.4 Statistical analysis

Following coding and tabulation, the data were statistically analyzed. A one-way analysis of variance (ANOVA) test was employed to compare the variables across the categories.

3. Results

3.1 Histologic features

3.1.1 Group I: (control group)

The parotid salivary gland is composed of secretory end pieces and a duct system. The acini were detected to consist of pyramidal-shaped serous cells with round, deeply basophilic nuclei. The intercalated ducts are difficult to identify as they are compressed between the secretory units, while the striated duct cells were tall columnar with basal striation. All these structures are arranged in lobes and lobules separated by connective tissue septa Fig (1).

3.1.2 Subgroup (A): (cisplatin group)

3.1.2.1 Histologic features at 7 days

The lobes appeared apart from each other with large spaces while the acini appeared vacuolated and shrunken. The striated duct cells showed loss of their cellular boundaries and striations and their cytoplasm showed vacuolization and degeneration Fig (2).

3.1.2.2 Histologic features at 21 days

The results revealed that the acini are completely shrunken with ill distinct acinar boundaries and vacuolation of the cytoplasm, while the striated ducts showed complete loss of their architecture and cytoplasm showing degeneration criteria Fig (3).

3.1.3 Subgroup (B): (BMMSC group)

3.1.3.1 Histologic features at 7 days

The specimen revealed that the normal structure features of the gland were generally preserved as evidenced by regular arrangement of secretory acini and ducts. However, some acini appeared with vacuolated cytoplasm. Ducts showed columnar cells with basally situated nucleus and ill distinct cell boundaries with vacuolated cytoplasm fig (4).

3.1.3.2 Histologic features at 21 days

The spherical fashion of acini was preserved with less vacuoles and distinct cell boundaries. Striated ducts appear close to normal with basal striation and mitotic division with open faced vesicular nucleus. Multiple patent blood vessels were seen around the ducts. Fig. (5).

3.2 Electron microscopic investigations

3.2.1 Group I: (control group)

The secretory acinar cells appeared as pyramidal shape structures. They connected with each other by cell-to-cell junctions in the form of tight junctions, gap junctions and desmosomes. The secretory units exhibited basally located nuclei and a relatively homogenous apical and supranuclear electron dense secretory granules embedded with the cytoplasm, they have a highly developed regularly arranged RER and elongated mitochondria (Fig.6).

3.2.1.1 Subgroup(A): (cisplatin group)

3.2.1.1.1 Electron microscopic investigations at 7 days

Showing severe alterations in the form of atrophic, fragmented and vacuolated acinar cells, also the cell junctions become ill defined. The nucleus appeared rounded in some cases and located basally, the cytoplasm appeared laden with dense electron secretory granules which have different size and density. RER showing deteriorative changes as they appear decreased in number with abnormal shape and arrangement, also rounded and sometimes flat shaped mitochondria was seen in the cytoplasm with decreased in their number. The ductal cells appear devoid from most of cell organelles Fig (7).

3.2.1.1.2 Electron microscopic investigations at 21 days

Showing that the acini were atrophic with pyknotic and shrunken nuclei, having different size and shape with irregular nuclear membrane and multiple cytoplasmic vacuoles. RER decreased in number and fragmented, swollen and decrease number of mitochondria were

observed. Different size and densities of electron dense secretory granules were seen while some areas showing a little or devoid of secretory granules Fig (8).

2.2.1.2 Subgroup (B): (BMMSC group)

2.2.1.2.1 Electron microscopic investigations at 7days

Showing the acinar cells appeared with some alterations as indistinct cell junctions, some acinar cells showing vacuolated cytoplasm. The RER appeared parallel and regularly arranged in most of specimens forming a network of saculles, while some specimen showing some areas of fragmented RER. The nucleus showing normal rounded shape, the cytoplasm contains electron dense granules of different size and density. The mitochondria appeared with different size with normal cisternae Fig (9).

2.2.1.2.2 Electron microscopic investigations at 21 days

The acinar cells appeared close to normal, the secretory acinar cells appeared as pyramidal shape structures, they connected with each other by cell-to-cell junctions in the form of tight junctions, gap junctions and desmosomes, the acinar cell cytoplasm contain all organelles, the cytoplasm contains a great number of different size and densities of electron dense secretory vesicles. The nucleus appeared with normal shape and surrounded by a well-arranged network of parallel RER, the mitochondria were seen distributed throughout the cytoplasm, the cytoplasm appeared devoid of cytoplasmic vacuolations Fig. (10).

4. Discussion

Chemotherapy is a critical component in the systemic management of salivary gland cancers, particularly those affecting the parotid glands (approximately 80%), accompanied by the submandibular and sublingual glands [11]. Cisplatin is extensively utilized and regarded as a highly effective chemotherapeutic agent for a variety of head and neck and ovarian tumors [12]. Despite its potent chemotherapeutic properties, Cisplatin may induce certain negative effects due to its cytotoxic nature and inability to selectively target cancer cells; it also impacts healthy tissues [1]. Functional and morphological degradation of salivary gland tissue may result from cisplatin treatment, which may cause the following side effects: disrupted production of saliva, swallowing dysfunctions, speech and taste issues, oropharyngeal discomfort, and infections of the oral cavity [13]. This research was conducted in order to counteract the detrimental impacts of cisplatin on healthy cells. Adult males of the Sprague-Dawley rats were selected for the research due to their small size, cleanliness, gentleness, ease of housing, handling, and rapid growth [14]. After 7 days, the histological and ultrastructural findings in the cisplatin group indicated that the acini were entirely diminished, exhibiting significant interlobular spaces. These findings were found to be coincidental with the research conducted by Shaymaa M. et al., who stated that the cisplatin group exhibited noticeable reductions in the size of glandular lobules and serous acini, along with interstitial oedema and numerous cytoplasmic vacuoles [15]. The current work revealed the presence of intra-cytoplasmic vacuoles ranging from small to large vacuoles; this work is

coincidental with Conklin KA., who postulated that this vacuolation attributed to the released free radicals from cisplatin causes damage to several cellular components [16]. Moreover, Terzi et al. stated that vacuoles may be a result of intensified acinus cell degeneration and apoptosis triggered by cisplatin administration [17].

The current findings revealed that most nuclei exhibited indications of degeneration. This observation was explained by J. Levi that the mechanism of action of cisplatin, which is activated upon entry into the cell and relocated by water molecules that replace the chloride atoms on cisplatin. The resulting hydrolyzed product may subsequently interact with any nitrogen donor atom on the nucleic acid, resulting in DNA damage, inhibition of cell division, and non-selective apoptosis that impacts both tumor and normal cells [18]. In addition, this may shed light on the observed alternations in the nucleus, such as fragmented and degenerated nuclei, as well as those with an irregular nuclear membrane and variations in size and shape. The present investigation conducted in the cisplatin group observed enlarged mitochondria that diminished or disappeared after 21 days. This finding is consistent with the research of J. Levi, who reported that the maximum concentration of cisplatin was detected in the mitochondria (37%) following cisplatin application [18]. The presence of lysosome engulfing secretory granules, mitochondria, and other organelles agreed with the study by Kitashima, who found lysosome-like bodies on the 5 days of CDDP infusion, and their number increased during the study. He demonstrated that auto phagocytosis in acinar cells is the first step toward recovery through digestion of cellular contents damaged by CDDP [19]. The present study observed numerous macrophages interspersed among atrophied, degenerated acini in the cisplatin group. Macrophages are crucial regulators of the local inflammatory environment [20] and are involved in the regeneration of tissue and inflammation [21]. The outcomes proved striated and excretory duct dilation accompanied by secretion stagnation. These results align with those of Eman Hany et al., who reported similar results. This may be attributed to the pathological impact of chemotherapy on myoepithelial cells, which embracing the EDs and prevent the secretion from being expelled into the oral cavity [22].

In contrast to the cisplatin group, the BMMSCs group exhibited superior histological outcomes, as evidenced by a discernible reduction in acinar vacuolation and nuclear degeneration. The therapeutic impact of BMMSC is demonstrated by the absence of vacuoles in serous acini, intercalated, striated, and excretory ducts, the presence of open-faced nuclei, mitotic division, numerous mitochondria, and a well-organized RER, in comparison to the other group. Following seven days, the lobules exhibited acini with typical features and an open-faced vesicular nucleus. These outcomes agreed with those of Tran et al., who introduced BMSCs into the tail veins of rats with irradiated submandibular glands. Furthermore, Tran et al. identified improved functioning of the submandibular glands, elevated proliferation, diminished apoptosis, and enhanced vascularity [23].

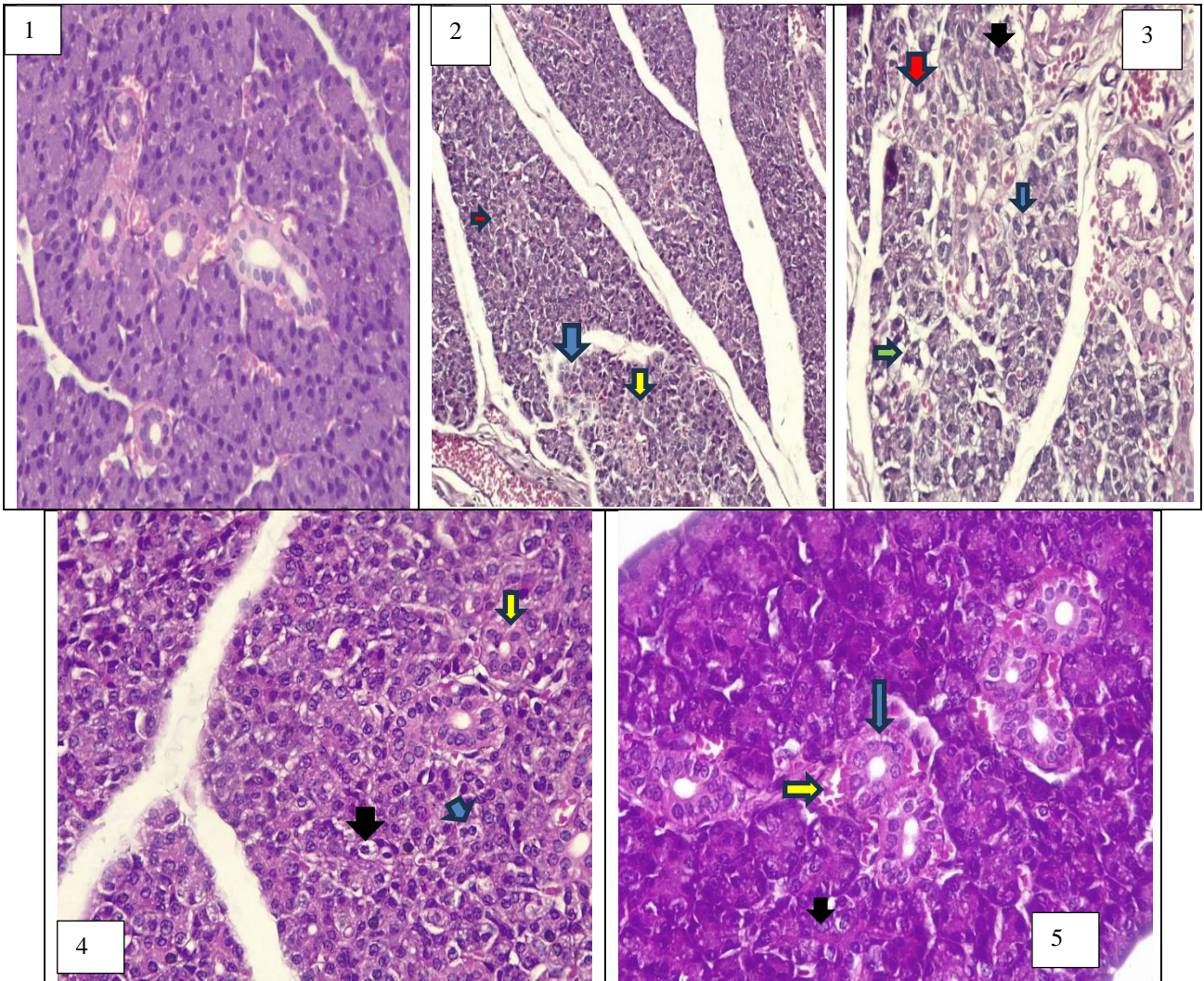


Figure 1: The parotid salivary gland of a rat from the control group reflected normal serous acini with deep eosinophilic cytoplasm and deep basophilic nucleus. At the same time, some collecting ducts lie among serous acini (H&E, X400).

Figure 2: cisplatin group at 7 days showing a- necrosis between atrophied acini(blue) b-atrophied striated duct with degenerated cytoplasm (yellow) c- acinar vacuoles(red) (H&E, X 400).

Figure 3: cisplatin group at 21 showing a- striated duct with vacuolation and degeneration(red) b- nuclear karyolysis (green) c-acinar vacuolation (blue) d- macrophage(black) (H&E, X 400).

Figure 4: stem cell group at 7 days showing a striated duct with some vacuoles(yellow) b- mitotic figures(blue) c- vacuolated acini (black) (H&E, X400).

Figure 5: stem cell group at 21 days showing a- new blood vessels around ducts(yellow) b- striated duct with apparent basal striation(blue) and open-faced nuclei (black) (H&E, X400)

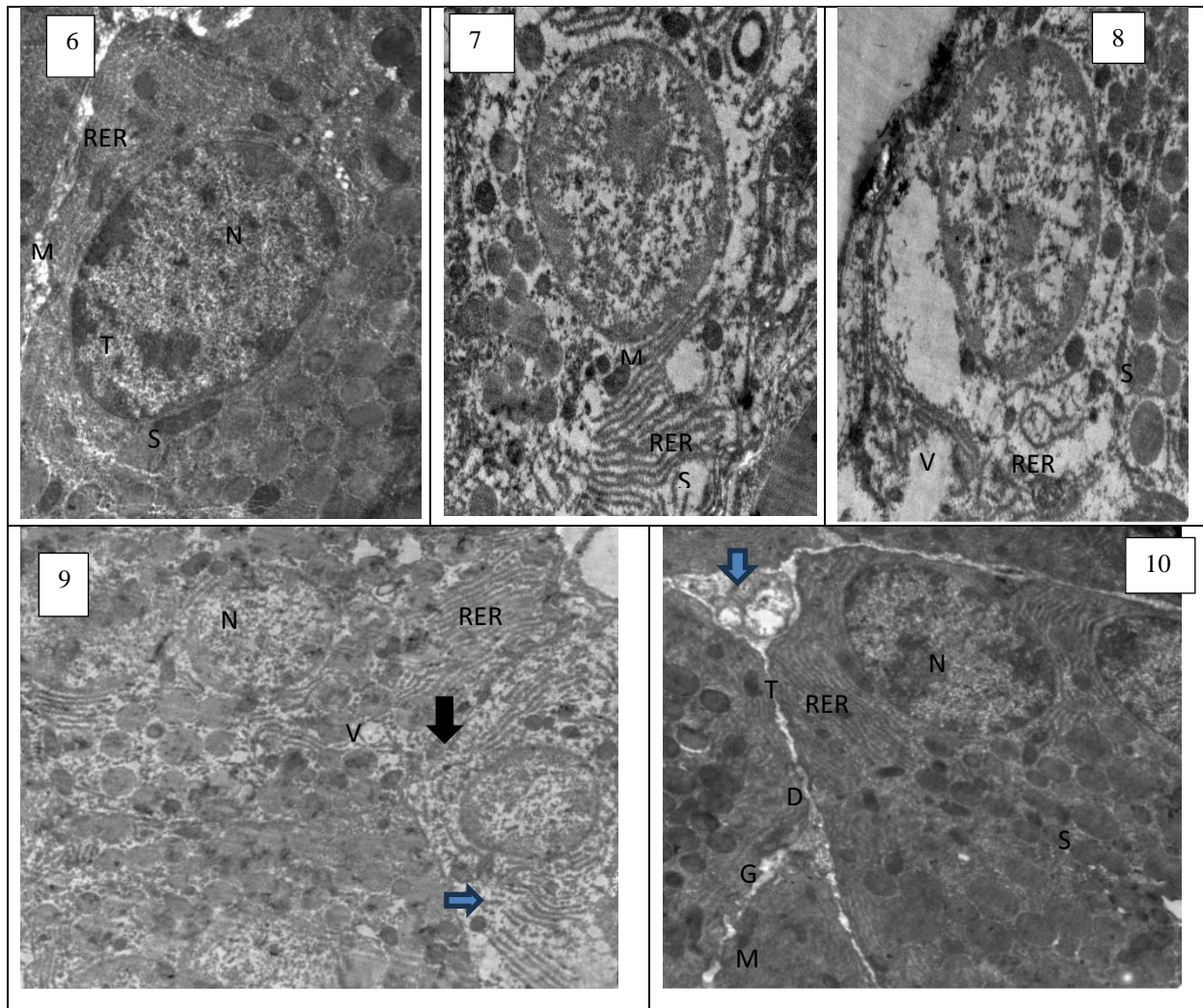


Figure 6: Electron micrographs of parotid glands of control group showing the nucleus (N), cisternae of RER, mitochondria(M), tight junction (T) and electron dense secretory granules (S) (X15000).

Figure 7: Electron micrographs of parotid glands of cisplatin group at 7 days showing a- dilated and fragmented RER b- few secretory granules (s) c- flat shaped mitochondria(M) (X15000).

Figure 8: Electron micrographs of parotid glands of cisplatin group at 21 days showing a- coiled RER b- vacuolated cytoplasm (V) c- secretory granules with different size(S) (X15000).

Figure 9: Electron micrographs of parotid glands of stem cell group at 7 days showing a- rounded nucleus b- well-arranged RER (red) and fragmented in some areas (blue) c- indistinct cell junctions (black) d- vacuolation (v) (X8000).

Figure 10: Electron micrographs of parotid glands of stem cell at 21 days showing a- nucleus b- RER c- mitochondria d- lumen contain secretory secretion (blue) e- cell junction (T, G, D) f- secretory granules (X10000).

Table 1: Comparison between Cisplatin, stem cell and control group regarding the percentage of area of intracytoplasmic vacuolations due to glands atrophy at 7 and 21 days.

% area of intracytoplasmic vacuolations due to glands atrophy		Cisplatin group No. = 120	Stem cell group No. = 120	Control group No. = 120	Test value	-value	ig.
Day 7	Mean ± SD	1.93 22.68 ±	9.51 ± 0.97	4.47 ± 0.64	6264.018	0.01	S
	Range	17 – 28.5	7.1 – 11.8	2.6 – 6.4			
Day 21	Mean ± SD	3.04 28.05 ±	7.2 ± 0.77	4.47 ± 0.64	4479.008	0.01	S
	Range	21.2 – 36	5.5 – 9.3	2.6 – 6.4			
Post Hoc analysis							
		P1	P2	P3			
Day 7		<0.01	<0.01	<0.01			
Day 21		<0.01	<0.01	<0.01			

Non-significant (P-value > 0.05); Significant (P-value < 0.05); Highly significant (P-value < 0.01).

P1: Cisplatin Vs stem cell; **P2:** Cisplatin Vs control; **P3:** stem cell Vs control

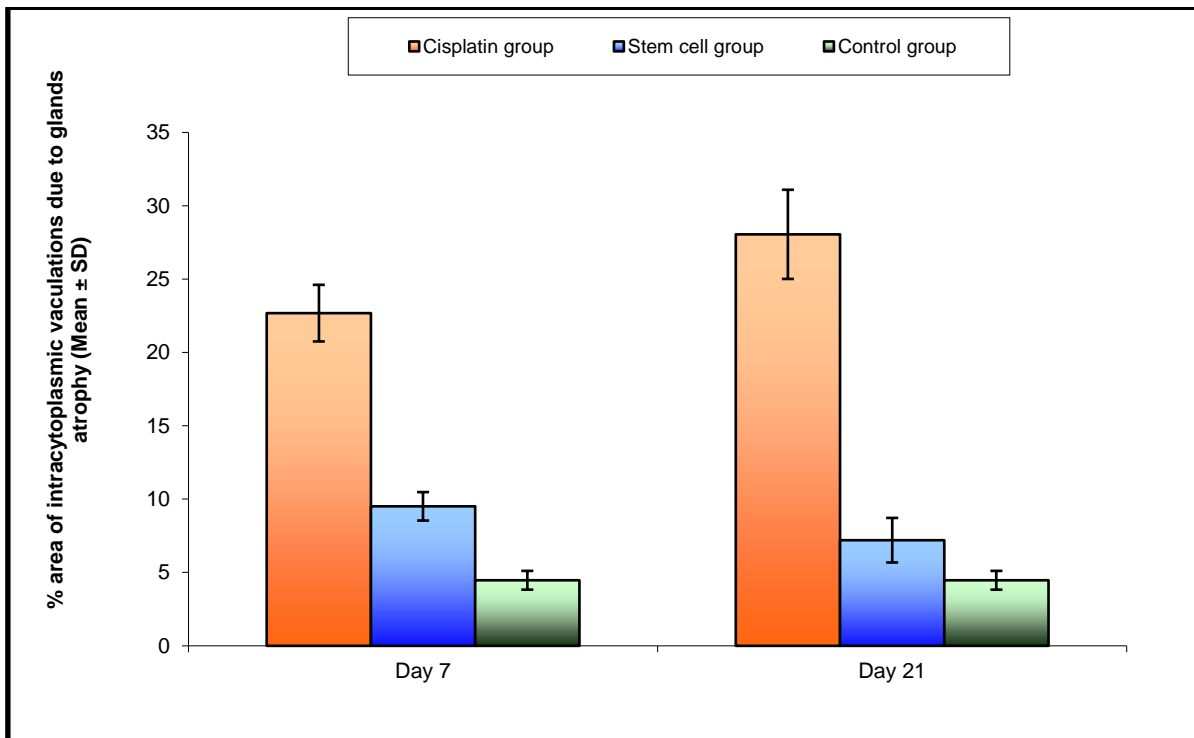


Figure 11: Comparison between Cisplatin, stem cell and control group regarding the percentage of area of intracytoplasmic vacuolations due to glands atrophy at 7 and 21 days.

Previous investigations examined the impact of local BMSC transplantation into the submandibular glands of irradiated mice and revealed that acinar cells and gland morphologies remained intact while gland functions, such as salivary flow rate and glandular weight, increased [24-25]. Wang et al., [26] observed no disparity in apoptosis and cellular proliferation between the Stem Cells group and the irradiated group, which contradicts our findings. In their research, 2×10^5 SCs/rat were administered intra-glandularly, whereas utilized 5×10^5 SCs/rat in the present investigation. A possible explanation for this discrepancy in findings is variations in the number of stem cells utilized in each investigation. The current work revealed improvement in the stem cell group after 21 days, as evidenced by fewer vacuoles and more distinct cell boundaries; the striated duct appeared normal, with basal striation and numerous patent blood vessels surrounding it. Coincidental with the findings of Lombaert et al., our results indicate that transplanted BMMCs can colonise injured SGs and stimulate repair processes via paracrine signalling, thereby enhancing glandular function and morphogenesis [27]. The observed decrease in apoptosis and a rise in microvessel density in the group treated with BMMSCs are likely attributable to the paracrine effects of BMMSC.

The results of this study align with a prior report that documented the enhanced regenerative tissue capabilities of SGs transplanted with BMMCs, including the formation of blood vessels and proliferation of cells [24]. In a murine hind-limb ischemia model, You et al. found that BMMSC treatment stimulated vasodilation, implying that the proangiogenic activity of MSCs might depend on their ability to modulate the function of pre-existing vessels [28].

5. Conclusion

The potential of BMMSc as a therapeutic intervention for cisplatin-induced cytotoxicity in the parotid gland of rats is worth considering. Additionally, BMMSc has been observed to augment the proliferative capacity and repair potential of parotid gland cells subsequent to cisplatin injection.

Declarations

Ethical Approval

All experiments were carried out at the house animals of veterinary medicine Cairo University and approved by the local ethical committee Ref. No.592/1786.

- Animals in each group were caged in separate cages.
- Animals were housed in an isolated building located as far away from human habitations as possible and not exposed to dust, smoke, noise, insects, and birds.
- The cages were made of suitable metal (stainless steel).
- The cage was suitable in size for the rats.
- The cages had adequate arrangement for feeding and watering.
- Room temperature was ranged from 22-24c to be suitable for the rats to avoid change in food and water intake.
- Rats were maintained on a balanced diet. A balanced diet contained protein, carbohydrates fat, minerals, vitamins, and water in required proportions for rats.
- Procedures which are considered painful were conducted under appropriate anesthesia.

Competing interests

No competing interests

Funding

No funding

Availability of data and materiales

All data used are original and available upon needed.

AFFI city cairo Egypt

AFF2city cairo Egypt

AFF3city cairo Egypt

References

- [1] S. Hitomi, I. Ujihara, M. Sago-Ito, T. Nodai, T. Shikayama, K. Inenaga, K. Ono. (2019). Hyposalivation due to chemotherapy exacerbates oral ulcerative mucositis and delays its healing. *Archives of oral biology*. 105: 20-26.
- [2] M. Crul, J. Schellens, J. Beijnen, M. Maliepaard. (1997). Cisplatin resistance and DNA repair. *Cancer treatment reviews*. 23(5-6): 341-366.
- [3] M. Crul, J. Schellens, J. Beijnen, M. Maliepaard. (1997). Cisplatin resistance and DNA repair. *Cancer treatment reviews*. 23(5-6): 341-366.
- [4] S. Qi, D. Wu. (2013). Bone marrow-derived mesenchymal stem cells protect against cisplatin-induced acute kidney injury in rats by inhibiting cell apoptosis. *International Journal of Molecular Medicine*. 32(6): 1262-1272.
- [5] J. Liu, H. Zhang, Y. Zhang, N. Li, Y. Wen, F. Cao, H. Ai, X. Xue. (2014). Homing and restorative effects of bone marrow-derived mesenchymal stem cells on cisplatin injured ovaries in rats. *Molecules and cells*. 37(12): 865.
- [6] B.R. Weil, T.A. Markel, J.L. Herrmann, A.M. Abarbanell, D.R. Meldrum. (2009). Mesenchymal stem cells enhance the viability and proliferation of human fetal intestinal epithelial cells following hypoxic injury via paracrine mechanisms. *Surgery*. 146(2): 190-197.
- [7] Y. Sumita, Y. Liu, S. Khalili, O.M. Maria, D. Xia, S. Key, A.P. Cotrim, E. Mezey, S.D. Tran. (2011). Bone marrow-derived cells rescue salivary gland function in mice with head and neck irradiation. *The international journal of biochemistry & cell biology*. 43(1): 80-87.
- [8] J.-Y. Lim, T. Yi, J.-S. Choi, Y.H. Jang, S. Lee, H.J. Kim, S.U. Song, Y.-M. Kim. (2013). Intraglandular transplantation of bone marrow-derived clonal mesenchymal stem cells for amelioration of post-irradiation salivary gland damage. *Oral oncology*. 49(2): 136-143.
- [9] A. Roldán-Fidalgo, S.M. Saldaña, A. Trinidad, B. Olmedilla-Alonso, A. Rodríguez-Valiente, J.R. García-Berrocal, R. Ramírez-Camacho. (2016). In vitro and in vivo effects of lutein against cisplatin-induced ototoxicity. *Experimental and Toxicologic Pathology*. 68(4): 197-204.
- [10] J. Jeong, H. Baek, Y.-J. Kim, Y. Choi, H. Lee, E. Lee, E.S. Kim, J.H. Hah, T.-K. Kwon, I.J. Choi.

- (2013). Human salivary gland stem cells ameliorate hyposalivation of radiation-damaged rat salivary glands. *Experimental & molecular medicine*. 45(11): e58-e58.
- [11] Y.G. Rochefort, P. Vaudin, N. Bonnet, J.-C. Pages, J. Domenech, P. Charbord, V. Eder. (2005). Influence of hypoxia on the domiciliation of mesenchymal stem cells after infusion into rats: possibilities of targeting pulmonary artery remodeling via cells therapies? *Respiratory research*. 6: 1-13.
- [12] F. Ito, K. Ito, P. Vargas, O. De Almeida, M. Lopes. (2005). Salivary gland tumors in a Brazilian population: a retrospective study of 496 cases. *International journal of oral and maxillofacial surgery*. 34(5): 533-536.
- [13] A.P. Venook, A. Tseng Jr, F. Meyers, I. Silverberg, R. Boles, K. Fu, C. Jacobs. (1987). Cisplatin, doxorubicin, and 5-fluorouracil chemotherapy for salivary gland malignancies: a pilot study of the Northern California Oncology Group. *Journal of Clinical Oncology*. 5(6): 951-955.
- [14] A.S. Al-Refai, A.K. Khaleel, S. Ali. (2014). The effect of green tea extract on submandibular salivary gland of methotrexate treated albino rats: Immunohistochemical study. *Journal of Cytology & Histology*. 5(2): 1.
- [15] M.F.d. Souza, N. Couto-Pereira, L. Freese, P.A. Costa, G. Caletti, K.M. Bisognin, M.S. Nin, R. Gomez, H.M.T. Barros. (2014). Behavioral effects of endogenous or exogenous estradiol and progesterone on cocaine sensitization in female rats. *Brazilian Journal of Medical and Biological Research*. 47: 505-514.
- [16] S.M. Dessoukey, A.M. Halawa, I.A. Fathy, D.M. Kashkoush. (2021). The Effect of Adipose Derived Stem Cells versus Platelet Rich Plasma in Ameliorating Cisplatin-Induced Injury on The Submandibular Salivary Gland.” *A Comparative Histological Study”*. *Egyptian Journal of Histology*. 44(2): 406-417.
- [17] K.A. Conklin. (2004). Chemotherapy-associated oxidative stress: impact on chemotherapeutic effectiveness. *Integrative cancer therapies*. 3(4): 294-300.
- [18] S. Terzi, A. Özgür, T. Mercantepe, M. Çeliker, L. Tümkaya, E. Dursun. (2017). The effects of astaxanthin on salivary gland damage caused by cisplatin in the rat. *Int J Res Med Sci*. 5(4): 1410-1414.
- [19] J. Levi, C. Jacobs, S. Kalman, M. McTigue, M. Weiner. (1980). Mechanism of cis-platinum nephrotoxicity: I. Effects of sulfhydryl groups in rat kidneys. *Journal of Pharmacology and Experimental Therapeutics*. 213(3): 545-550.
- [20] S. Kitashima. (2005). Morphological alterations of submandibular glands caused by cisplatin in the rat. *The Kurume medical journal*. 52(1+ 2): 29-38.
- [21] S. Zhang, Y. Liu, X. Zhang, D. Zhu, X. Qi, X. Cao, Y. Fang, Y. Che, Z.-C. Han, Z.-X. He. (2018). Prostaglandin E2 hydrogel improves cutaneous wound healing via M2 macrophages polarization. *Theranostics*. 8(19): 5348.
- [22] W. Li, X. Zhang, F. Wu, Y. Zhou, Z. Bao, H. Li, P. Zheng, S. Zhao. (2019). Gastric cancer-derived mesenchymal stromal cells trigger M2 macrophage polarization that promotes metastasis and EMT in gastric cancer. *Cell death & disease*. 10(12): 918.
- [23] E. Hany, M.A. Sobh, M.T. Abou ElKhier, H.M. ElSabaa, A.R. Zaher. (2017). The effect of different routes of injection of bone marrow mesenchymal stem cells on parotid glands of rats receiving cisplatin: a comparative study. *International journal of stem cells*. 10(2): 169-178.
- [24] S.D. Tran, Y. Sumita, S. Khalili. (2011). Bone marrow-derived cells: a potential approach for the treatment of xerostomia. *The international journal of biochemistry & cell biology*. 43(1): 5-9.
- [25] Y. Sumita, Y. Liu, S. Khalili, O.M. Maria, D. Xia, S. Key, A.P. Cotrim, E. Mezey, S.D. Tran. (2011). Bone marrow-derived cells rescue salivary gland function in mice with head and neck irradiation. *The international journal of biochemistry & cell biology*. 43(1): 80-87.
- [26] T. Kojima, S.i. Kanemaru, S. Hirano, I. Tateya, S. Ohno, T. Nakamura, J. Ito. (2011). Regeneration of radiation damaged salivary glands with adipose-derived stromal cells. *The Laryngoscope*. 121(9): 1864-1869.
- [27] Z. Wang, H. Xing, H. Hu, T. Dai, Y. Wang, Z. Li, R. An, H. Xu, Y. Liu, B. Liu. (2018). Intraglandular transplantation of adipose-derived stem cells combined with platelet-rich fibrin extract for the treatment of irradiation-induced salivary gland damage. *Experimental and Therapeutic Medicine*. 15(1): 795-805.
- [28] I.M. Lombaert, P.K. Wierenga, T. Kok, H.H. Kampinga, G. dehaan, R.P. Coppes. (2006). Mobilization of bone marrow stem cells by granulocyte colony-stimulating factor ameliorates radiation-induced damage to salivary glands. *Clinical Cancer Research*. 12(6): 1804-1812.
- [29] D. You, L. Waeckel, T.G. Ebrahimian, O. Blanc-Brude, P. Foubert, V. Barateau, M. Duriez, S. LeRicousse-Roussanne, J. Vilar, E. Dejana. (2006). Increase in vascular permeability and vasodilation are critical for proangiogenic effects of stem cell therapy. *Circulation*. 114(4): 328-338.